PNAS RESEARCH ARTICLE | ECOLOGY OPEN ACCESS

Plants maintain climate fidelity in the face of dynamic climate change

Yue Wang[a,b,1], Silvia Pineda-Munoz[c,b,d], and Jenny L. McGuire[b,e,f]

Edited by Nils Stenseth, Universitetet i Oslo, Oslo, Norway; received March 14, 2022; accepted July 22, 2022

Plants will experience considerable changes in climate within their geographic ranges over the next several decades. They may respond by exhibiting niche flexibility and adapting to changing climates. Alternatively, plant taxa may exhibit climate fidelity, shifting their geographic distributions to track their preferred climates. Here, we examine the responses of plant taxa to changing climates over the past 18,000 y to evaluate the extent to which the 16 dominant plant taxa of North America have exhibited climate fidelity. We find that 75% of plant taxa consistently exhibit climate fidelity over the past 18,000 y, even during the times of most extreme climate change. Of the four taxa that do not consistently exhibit climate fidelity, three—elm (*Ulmus*), beech (*Fagus*), and ash (*Fraxinus*)—experience a long-term shift in their realized climatic niche between the early Holocene and present day. Plant taxa that migrate longer distances better maintain consistent climatic niches across transition periods during times of the most extreme climate change. Today, plant communities with the highest climate fidelity are found in regions with high topographic and microclimate heterogeneity that are expected to exhibit high climate resilience, allowing plants to shift distributions locally and adjust to some amount of climate change. However, once the climate change buffering of the region is exceeded, these plant communities will need to track climates across broader landscapes but be challenged to do so because of the low habitat connectivity of the regions.

climatic niche | migration | plants | biogeography | paleoecology

Significance

Seventy-five percent of plant taxa have consistently shifted their geographic distributions to track their preferred climates over the past 18,000 years. These same plants will likely need to do the same today, given the magnitude of recent climate change. However, they may be limited in their ability to do so due to habitat fragmentation and rapidly changing climates.

Climate is an important abiotic factor in determining why species live where they do (1–5). When climate changes, we anticipate that species may be forced to shift their geographic distributions to track their climatic niches across the landscape (1, 6). However, climate tracking can only serve as a hypothesis for species' anticipated range changes, because, in addition to climate, many other factors play a role in range dynamics, including interspecific interactions, dispersal ability, land use, soil, topography, and historical occurrences (7–9). In contrast, several studies have suggested that, rather than shifting their geographic distributions to track climates, some animal and plant species have exhibited climatic niche shifts over long timescales (10–12) or persisted by contracting their geographic ranges into refugia (13). Studying niche dynamics over thousands of years is important for understanding how species adapt to climate change, protecting species' habitats from environmental disturbances, and maintaining biodiversity under the rapid climate change in the centuries to come.

Plant taxa have experienced large range shifts as climates changed since the Last Glacial Maximum (~21 kya), and individual plant species shifted more rapidly and more stochastically than plant biomes or communities (9, 12, 14, 15). Given climate projections, we anticipate that plant biomes will experience considerable temperature changes within their current geographic ranges (16). However, plant species may not be able to migrate rapidly enough to track those changes across broad landscapes (6, 17). To understand the controls on species ranges and the future needs thereof, we must first understand the relationship between dispersal potential, plant characteristics, and realized climatic niches over time.

Here, we introduce climate fidelity, which evaluates the climatic niche dynamics of individual plant taxa to assess how well they have shifted their ranges to track their realized climatic niche as climate has changed. Taxa that exhibit climate fidelity maintain their niches and track climate change through time. Taxa that do not exhibit climate fidelity fail to track climate change geographically and instead shift their niches within the climatic space, adapting to or surviving despite local climate change. By assessing climate fidelity, we can characterize the flexibility of the realized climatic niches of individual taxa, revealing their movement needs and adaptive capacities in coming decades.

Our analyses initially assess whether each of 16 North American plant taxa exhibit climate fidelity over the past 18,000 y (*Methods*, Pollen datasets and *SI Appendix*, Table S1). These plant taxa include 12 tree taxa (from the most abundant to the least

Author affiliations: [a]School of Ecology, Sun Yat-sen University, Shenzhen 518107, China; [b]School of Biological Sciences, Georgia Institute of Technology, Atlanta, GA 30332; [c]Amazon Conservation Association, Washington, DC 20005; [d]Department of Earth and Environmental Sciences, Indiana University, Bloomington, IN 47401; [e]School of Earth and Atmospheric Sciences, Georgia Institute of Technology, Atlanta, GA 30332; and [f]Interdisciplinary Graduate Program in Quantitative Biosciences, Georgia Institute of Technology, Atlanta, GA 30332

Author contributions: Y.W., S.P.-M., and J.L.M. designed research; Y.W. and J.L.M. performed research; Y.W., S.P.-M., and J.L.M. contributed new reagents/analytic tools; Y.W., S.P.-M., and J.L.M. analyzed data; and Y.W., S.P.-M., and J.L.M. wrote the paper.

The authors declare no competing interest.

This article is a PNAS Direct Submission.

[1]To whom correspondence may be addressed. Email: wangyue25@mail.sysu.edu.cn.

This article contains supporting information online at http://www.pnas.org/lookup/suppl/doi:10.1073/pnas.2201946119/-/DCSupplemental.

abundant)—pine (*Pinus*), oak (*Quercus*), spruce (*Picea*), birch (*Betula*), alder (*Alnus*), hemlock (*Tsuga*), cypress (Cupressaceae), beech (*Fagus*), elm (*Ulmus*), fir (*Abies*), ash (*Fraxinus*), and willow (*Salix*)—and four herb taxa—grass (Poaceae), sedge (Cyperaceae), sagebrush (*Artemisia*), and pigweed (Amaranthaceae). Taxonomy is decided based on the level of pollen identification and include 12 genera and 4 families (*SI Appendix*, Fossil pollen dataset). We include these 16 of 64 possible plant taxa from the pollen records, as their average abundances per sample are ≥1%. Together, these taxa compose 83.3% of pollen grains in all pollen samples. To reconstruct realized climatic niches and geographic ranges, pollen data are pooled into four time bins that are 4,000 y in length from 18 ka until 2 ka (thousands of years before present, where present is 1950 AD) and two shorter time bins (2 ka to 1950 AD and 1950 AD to present) to examine recent times at a higher temporal resolution (Fig. 1 and *SI Appendix*, Fig. S1). By comparing adjacent time bins, we estimate changes that occurred across five transition periods (Fig. 1). For example, the deglaciation transition period (DG) examines changes between the 18–14 ka bin and the 14–10 ka bin (see Fig. 1 for all time bins and transition periods). The six time bins represent specific climate scenarios, and each period is sufficiently long for most plants to migrate and track their preferred climates (18).

We define climate fidelity as a taxon's ability to exhibit significant realized climatic niche similarity (19–21) (*Methods*, Niche similarity) through time. We further diagnose the validity of this metric by comparing it with niche overlap values between transition periods (Schoener's *D*; *Methods*, Niche overlap) (19–21) and evaluating whether geographic range centroids shift synchronously with climate change. By incorporating range change dynamics, we test the hypothesis that the taxa that have historically migrated the most were able to maintain more static niches, effectively maintaining climate fidelity. After calculating the climate fidelity of each taxon, we examine the ecological and phenotypic characteristics of plants that exhibit higher climate fidelity. We test the hypothesis that plants with propensities for warmer, more-arid climates will exhibit higher climate fidelity due to their ability to migrate across harsher climatic conditions during the drought event of the middle Holocene (22). The idea to assess plant dynamics and climate fidelity resulted from years of discussion with conservation organizations, including The Nature Conservancy. For our final analyses, we create climate fidelity hotspots exhibited by each taxon within a modern plant community. Using these hotspots, together with climate resilience layer from The Nature Conservancy, we test what landscapes will hold for these plants that need to adjust to changing climates. Locations that exhibit climate resilience, high topoclimate complexity, and local connectivity are proposed to have greater potential to support adaptive, short-distance movements of taxa in response to climate drivers, because they provide local access to a range of climatic microsites (13, 23, 24). We finally assess the regional connectivity/nonconnectivity of these hotspots. Climate fidelity hotspots may require more conservation efforts to facilitate species migration because more taxa will need to disperse to track changing climates in the future.

Results and Discussion

The Climate Fidelity of Plants. North American plants have demonstrated consistent climate fidelity over the last 18,000 y, even during periods of climate change. Plant taxa exhibited climate fidelity across transition periods 86% of the time, even using a high-confidence threshold ($P \leq 0.01$) for climate fidelity. Seventy-five percent of plant taxa exhibited climate fidelity across all transition periods (at $P \leq 0.05$ significance level), and 50% of plant taxa have consistently high confidence ($P \leq 0.01$) of climate fidelity (Fig. 2*A* and *SI Appendix*, Fig. S2 and Table S2). Low climate fidelity is only exhibited during the DG and early Holocene transition periods (Fig. 2 *A* and *B*), when climate is changing most. This aligns with community-level plant-climate mismatches identified by Knight et al. (12) using eastern North American pollen assemblages.

Previous palynological studies propose that plants can disperse a long distance over uninhabitable landscapes and track climatic conditions on continental scales (2, 25, 26). Our analysis statistically supports this perception in most plant taxa, demonstrating that most plants can track their preferred climate on the continental scale without shifting their realized climatic niches. Our findings also reflect those of Antell et al. (27), who find that foraminifera (unicellular shelly protists) have consistently exhibited static-realized thermal niches over

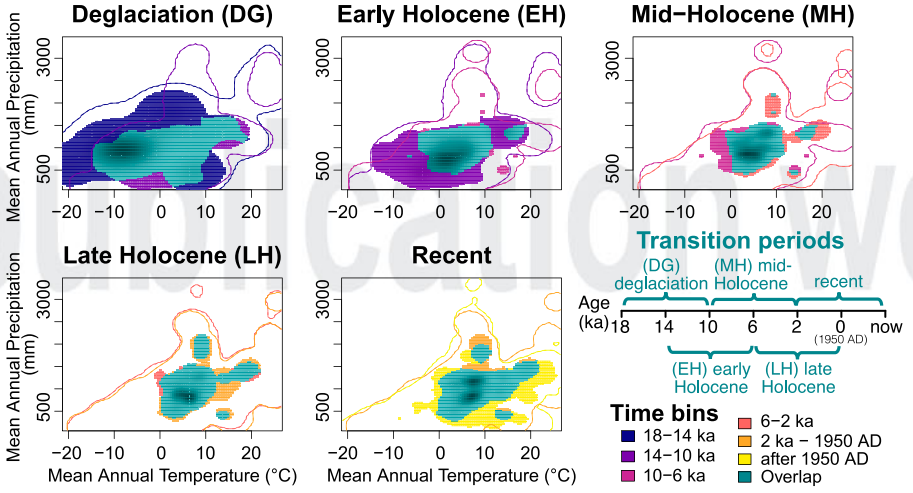

Fig. 1. Study design. We reconstruct the realized climatic niche for six time bins (*Bottom-right* panel) for each taxon. We calculate the niche overlap and climate fidelity of 16 North American plant taxa over five transition periods (*Bottom-right* panel, teal text): deglaciation (DG) (18–14 to 14–10 ka), early Holocene (EH) (14–10 to 10–6 ka), mid-Holocene (10–6 to 6–2 ka), late Holocene (6–2 to 2–0 ka), and recent (2–0 ka to after 0 ka, where 0 ka is 1950 AD) (19–21, 57, 58). The example shows the niche overlap of ash (*Fraxinus*). Teal-colored regions indicate the niche overlap across transition periods, colored outlines indicate the background (or available) climate for each age bin, and all other filled colored regions indicate the realized climatic niche of ash in each age bin.

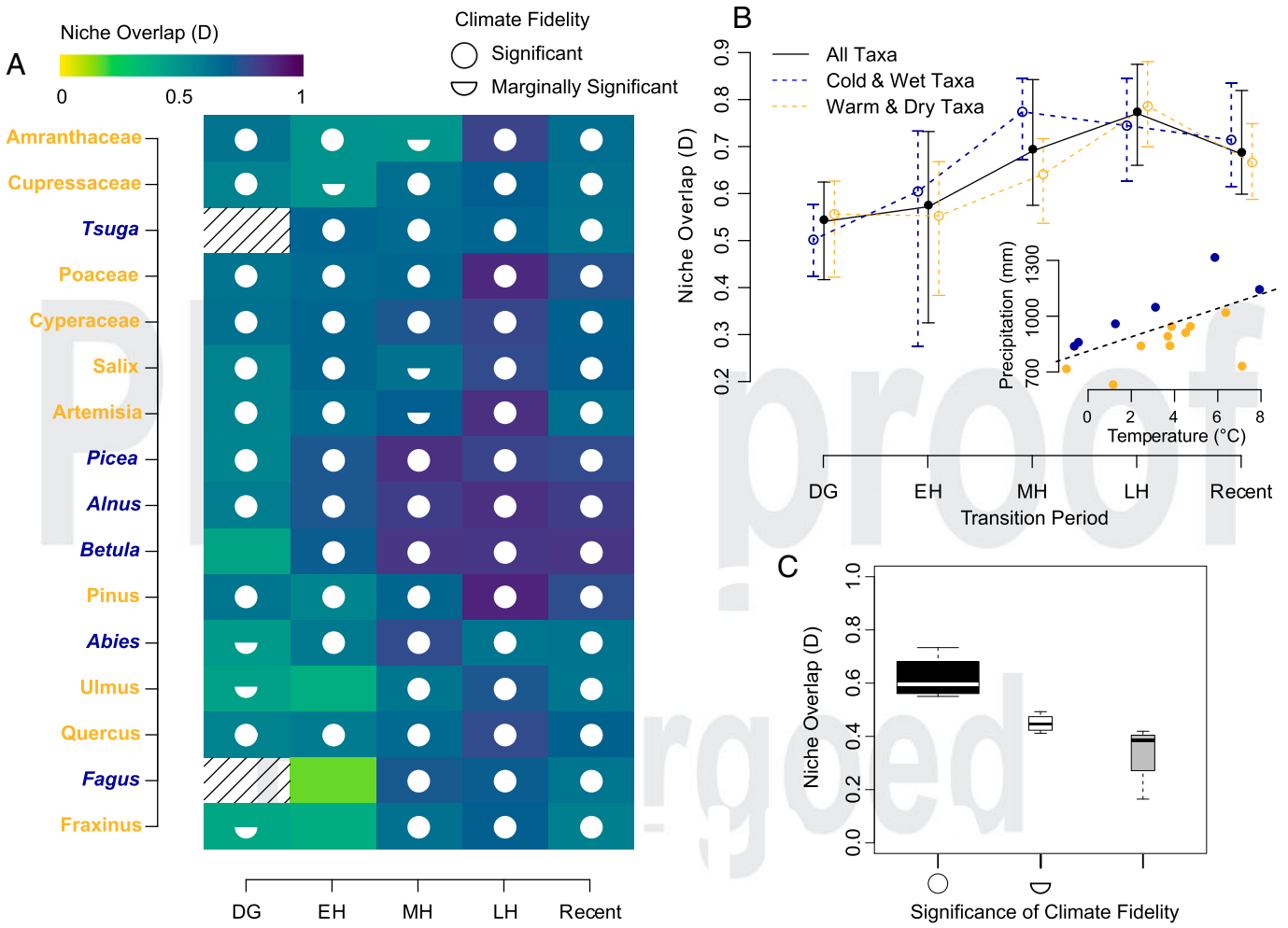

Fig. 2. The niche overlap and climate fidelity of plant taxa across transition periods (Fig. 1). (*A*) All plant taxa are listed along the *y* axis, ordered by migration distance from the longest (*Top*) to the shortest (*Bottom*). Plant taxon names are colored according to their affiliation with cold and wet climates (blue) versus warm and dry climates (gold). Colored boxes indicate climatic niche overlap (*D*) for each transition period. Climate fidelity significance based on niche similarity is indicated by white circles. Solid circles indicate significant results ($P \leq 0.01$), half circles indicate marginally significant results (between $P > 0.01$ and $P \leq 0.05$), no circle indicates no climate fidelity ($P > 0.05$), and hashed lines indicate low sample sizes ($n < 50$). (*B*) The average (point) and 90% confidence level (error bar) of all plant taxa (black), cold and wet taxa (blue), and warm and dry taxa (gold) across the five transition periods. The inset panel shows the mean scaled values of temperature and precipitation of plant taxa, where the dashed line indicates the ratio 0.5. (*C*) A box plot of niche overlap when compared with significant (open circle), marginally significant (half circle), and nonsignificant (blank) climate fidelity. All box plots are significantly different ($P < 0.01$).

the past 700 ka. That some plant taxa do not exhibit climate fidelity at times of most extreme change may be an indication of lag due to low dispersal speeds, spatial competition, or the presence of dispersal barriers, all of which are less of an issue for foraminifera in an open-ocean environment.

Elm, beech, ash, and birch were the only genera to exhibit periods of low climate fidelity. For elm, beech, and ash, low climate fidelity occurred during the early Holocene, and for birch, it occurred during the DG (Fig. 2*A* and *SI Appendix*, Fig. S2 and Table S2). Elm, beech, and ash exhibit a persistent lack of niche similarity and low overlap values when we compare the 18–14 ka time bin with the most recent time bin (after 1950 AD) (*SI Appendix*, Fig. S3 and Tables S3 and S4), indicating that there was a significant shift in their realized climatic niches during the Holocene. Birch, however, exhibited a difference in realized climatic niche only during the DG (*SI Appendix*, Tables S3 and S4). It demonstrates significant niche similarity for all other time periods (*SI Appendix*, Tables S3 and S4), indicating that the lack of climate fidelity during the DG was likely due to a lag in full recolonization following glacial retreat. Although it was once thought that birch exhibited rapid, long-distance dispersal (LDD) following glacial retreat, recent work has demonstrated that birch was in fact relegated to several small, remote refugia, from which it would have taken some time to fully re-expand while competing with secondary succession species (28–30). A genus-level summarization of range-filling analyses by Selinger et al. (31) (*SI Appendix*, Table S5) demonstrates that, relative to other taxa, all four of these plant taxa fill their modern potential ranges, estimated by modeling each species' distribution based upon their current realized climatic niches. The high range filling in birch implies that, following its postglacial re-expansion, it has maintained a relatively stable, now largely geographically occupied (range filling = 59%), realized climatic niche. In contrast, elm, beech, and ash have greatly reduced realized climatic niches, indicating a likely loss of adaptive capacity. Both elm and ash are thought to have experienced trophically induced niche changes as a result of megafaunal extinction, having been outcompeted by other tree taxa that were no longer being consumed and controlled by megafauna herbivores (32). However, for beech, some studies have indicated that the taxon may suffer from a detection issue in the middle Holocene (33, 34), which could affect realized climatic niche reconstructions.

Niche Overlap and Changing Climates. Overall, plant taxa show consistently high realized climatic niche overlap across transition periods for the last 18,000 y (mean ± SD: $D = 0.65 \pm 0.13$, Fig. 2*A* and *SI Appendix*, Fig. S4 and Table S6). The amount of realized climatic niche overlap that a plant taxon exhibited across time periods is highest in cases of high-confidence climate fidelity ($D = 0.69 \pm 0.09$), intermediate in cases of marginal-confidence climate fidelity ($D = 0.52 \pm 0.11$), and lowest in cases not exhibiting climate fidelity ($D = 0.34 \pm 0.12$) (Fig. 2*C*). All climate fidelity significance levels have significantly different niche overlap values ($P \leq 0.01$). Hereafter, we use niche overlap as a metric for exploring the timing and correlates of climate fidelity.

Plants with warmer, drier climatic niches exhibited the highest climatic niche overlap following the 4.2 ka drought event in North America (35, 36). However, the overall magnitude of background climate change does not correlate with plants' niche overlap (linear regression: mean of Pearson coefficient for temperature: $r = -0.18 \pm 0.42$, mean of Pearson coefficient for precipitation: $r = -0.18 \pm 0.29$, *Methods*, Niche overlap and climate change, *SI Appendix*, Table S7). To evaluate how plant climate propensity affects climate fidelity, we divide the plant taxa into two groups—cold, wet taxa and warm, dry taxa—based on their climatic niches from the past 18,000 y (*Methods*, Plant climate propensity, Fig. 2*B* and *SI Appendix*, Table S8). Results show that cold and wet taxa (e.g., hemlock and beech; Fig. 2*A*) reached their highest niche overlaps in the mid-Holocene before the 4.2 ka drought event ($D = 0.77 \pm 0.08$; Fig. 2 *A* and *B*). Warm and dry taxa (e.g., sagebrush and grass; Fig. 2*A*) exhibited the highest niche overlaps in the late Holocene after the 4.2 ka drought event ($D = 0.79 \pm 0.07$; Fig. 2 *A* and *B*). All warm and dry taxa expanded their niches in 6–2 ka, while the niches of cold and wet taxa did not change significantly in 6–2 ka but constricted in 2–0 ka (*SI Appendix*, Fig. S4). Our result of realized climatic niche change is corroborated by previous studies demonstrating the declines of cold, wet taxa after the 4.2 ka drought event (e.g., 37, 38) and increases in warm and dry taxa during the event (e.g., 39, 40). Our work implies that the timing of the highest climate fidelity may be driven by the climate propensity of the taxon.

Our results show that oak, pine, and spruce exhibited high climate fidelity through time (Fig. 2*A*). This might be caused by a taxonomic bias in our analysis. The analyses were performed at the genus level. Oak, pine, and spruce include many species within each of their genera in North America. A higher no. of species within a genus may lead to a larger climatic niche and larger niche overlaps. However, our work also suggests significantly high climate fidelity in plant genera represented by a single species during the past 18,000 y (Fig. 2*A*) in North America, such as alder and hemlock. Thus, the high climate fidelity for alder and hemlock supports the robustness of our work, though the high climate fidelity for oak, pine, and spruce may need further analysis. The high climate fidelity of plants may also be biased by the coarse spatial climate data and the large geographic area that pollen records can reflect. The low spatial resolution in the climate simulation (0.5° × 0.5°) and the large geographic area where plants are possibly present relative to pollen reconstructions may average the abrupt changes in climate, leading to high niche overlaps in the transition periods. Further work with higher taxonomic resolution, more refined climate data, and more precise plants distributions may be needed to further explore these questions.

Migration and Climate Fidelity. Plants that migrated further maintained higher niche overlap but only during times of rapid climate change (Fig. 3). To test the hypothesis that more mobile plant taxa exhibited higher climate fidelity, we calculate the migration distances of all 16 plant taxa across all five transition periods (*Methods*, Migration distance). On average, plants migrated 320 km per transition period (*SI Appendix*, Table S9). We divide the plant taxa into two groups: long-migrating taxa with average migration distances > 320 km and short-migrating taxa with average migration distances < 320 km (Fig. 3*A*, *Inset*). Long-migrating taxa do not demonstrate higher niche overlaps than short-migrating taxa overall ($D = 0.68 \pm 0.05$ and $D = 0.62 \pm 0.08$, respectively; *t* test, $P = 0.104$; Fig. 3*B*). However, across the transition periods where they experienced substantial climate change, the DG and early Holocene, long-migrating taxa maintained significantly higher niche overlap ($D = 0.62 \pm 0.05$ versus $D = 0.50 \pm 0.15$; *t* test, $P = 0.033$; Fig. 3*C*). All four taxa that failed to demonstrate climate fidelity—elm, beech, ash, and birch—exhibited comparatively short average migration distances (<205 km; *SI Appendix*, Table S9), with ash exhibiting the shortest migration distance of any taxon (62 ± 26 km).

Long-distance migrations result in an improved ability to maintain constant realized climatic niches, supporting the idea that there would be a similar advantage for LDD, defined as a rare, extreme dispersal event over uninhabitable matrix by wind or other dispersal vectors (25, 26, 41). Previous analysis of fossil records and modern ecological experiments indicate that plant dispersal rates can be as far as 500–1,000 m y^{-1}, although only 1–5% of the seeds experience LDD (e.g., 25, 26). Our analysis indicates that, on average, North American plants migrated 320 ± 220 km across each transition period (~4 ka) on the continental scale. However, these distance calculations could be overturned by the detection of small, previously undetected refugia (e.g., 28, 29). LDD or even relatively long migrations can help plants migrate out of local refugia to fulfill their geographic potential based upon their climatic niches, facilitating climate fidelity even under climate change.

Climate Fidelity Hotspots. Climate fidelity hotspots are sites that today contain many plant taxa that exhibited strong climate fidelity over the last 18,000 y (*Methods*, Climate fidelity score; *SI Appendix*, Table S10). We find that these hotspots are concentrated in the Rocky Mountains and along the northern border of the contiguous United States (Fig. 4*A* and *SI Appendix*, Fig. S5), where the climate resilience is high due to low human impacts, high topographic complexity, and resultant diversities of local microclimates and soils (23, 24). Simultaneously, climate fidelity hotspots (top 25%, blue and cyan in Fig. 4*B*) demonstrate significantly higher resilience than the climate fidelity coldspots (bottom 25%, red and lime in Fig. 4*B* and *SI Appendix*, Fig. S6; *t* test: $P < 0.001$). Nevertheless, connected landscapes show significantly lower climate fidelity than disconnected landscapes (*SI Appendix*, Fig. S6; *t* test: $P = 0.02$). Approximately 24.7% of climate fidelity hotspots are in less intact landscapes, while only 10.5% climate fidelity coldspots are in fragmented landscapes. Climate fidelity hotspots contain many plants that will need to track their realized climatic niche in response to climate change. Local climate resilience means that these plants will initially be able to shift their distributions locally to adapt to some magnitude of impending climate change. However, once local climatic capacity is exceeded, disconnected landscapes surrounding these hotspots might prohibit plants from tracking climate change across broader spatial scales. In addition, as plants show low climate fidelity in the DG and early Holocene when climate changes

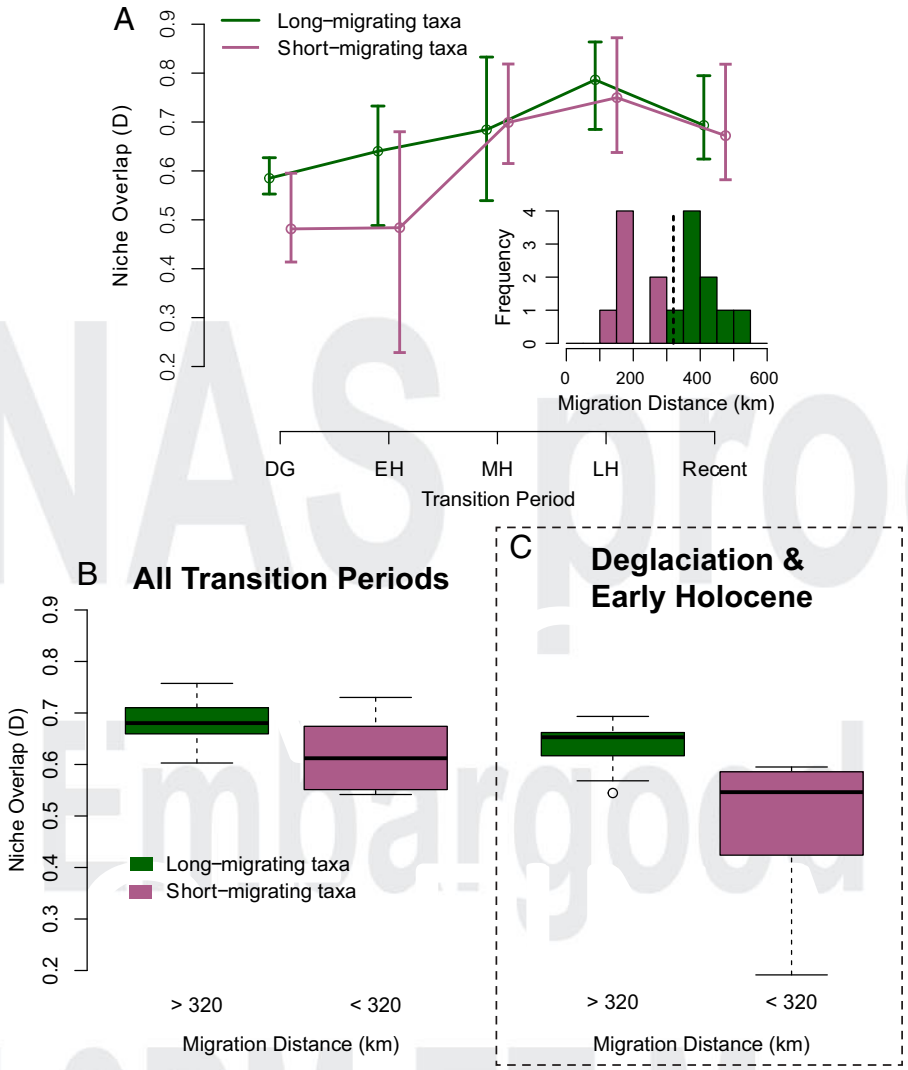

Fig. 3. Migration distances and niche overlap. (*A*) The niche overlap average (point) and 90% confidence level (error bar) of long-migrating plants (green) and short-migrating plants (purple) across the five transition periods. The inset panel shows the distribution of migration distance of all plant taxa, where the dashed line indicates the mean, 320 km. (*B*) The niche overlaps between long-migrating plants and short-migrating plant taxa over the last 18,000 y are not significantly different ($P = 0.104$). (*C*) However, long-migrating plant taxa show significantly higher niche overlaps during the deglaciation and early Holocene compared with short-migrating plant taxa ($P = 0.033$).

most, we may expect another decrease in climate fidelity in the near future, under accelerated climate change, due to dispersal limits or competition. Given anticipated expanded human activities over the next hundreds of years, migration facilitation, either through increased habitat connectivity or possibly even assisted migration, may be needed in the climate fidelity hotspots to help plants track climate change.

Conclusions

Most North American plant taxa have exhibited long-term climate fidelity over the past 18,000 y. Plant taxa that migrate further can track climate more effectively during periods of climate change but otherwise seem to track climate effectively over time. This supports the idea that slow-migrating taxa may lag modern, rapid changes in climate. However, there exists some climate buffering potential in regions where we find climate fidelity hotspots. Today, plant communities with high climate fidelity are found in regions with high climate resilience and low habitat connectivity. Plants in the most resilient regions can initially adapt to impending climate change by shifting their distributions locally. However, when the local climate change capacity is exceeded, plants will be challenged to track climate change due to lack of connectivity and human-induced habitat fragmentation. Steps toward facilitating migration are thus needed to help plants track their preferred realized climatic niches as climate changes in the future.

Methods

Pollen Datasets. We perform all analyses in R (42).

Surface and fossil pollen samples are sourced from the Neotoma Database (43, 44). Surface pollen samples are originally from the North American surface pollen dataset (45). Fossil pollen samples are from the recently compiled North American Bayesian-aged fossil pollen dataset (46, 47), see *SI Appendix*, Fossil pollen dataset), which has been integrated into Neotoma Database as a standalone chronology (43). We compile all pollen samples from 10°–80° N, 48°–140° W (which roughly corresponds to the North American continent) after 18 ka. We do not include pollen samples from Alaska (west of 140° W), due to the possible inaccuracies in the climate simulations in this region during DG (48, 49). In total, we compile 17,550 pollen samples, including 4,310 surface modern pollen samples and 13,240 fossil pollen samples from 337 sites (*SI Appendix*, Fig. S1 and Table S1). Please see *SI Appendix*, Fossil pollen dataset for a detailed description of the pollen samples used in this work.

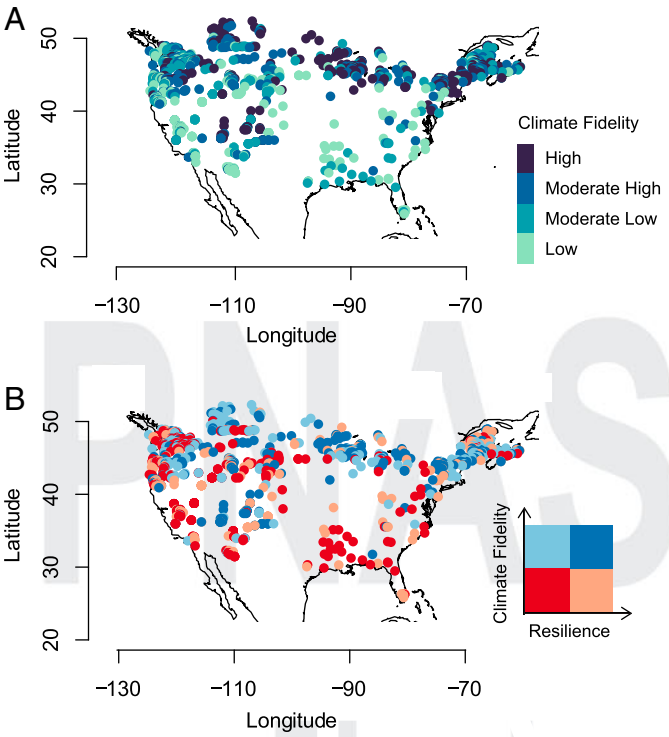

Fig. 4. Climate fidelity hotspots. (*A*) Quartiles of climate fidelity scores for modern pollen sites. (*B*) Climate fidelity hotspots (top quartile) and coldspots (lowest quartile) compared with local climate resilience (top and bottom quartiles). The Nature Conservancy's resilience score is based on current land use, topographic diversity, and local connectivity (64, 65).

We designate plant taxa as present or absent in the pollen samples using a set of abundance thresholds previously established using taphonomic processes (50, 51): *Pinus* as 5%; *Quercus*, *Betula*, and *Tsuga* as 2.5%; and all other taxa as 1%. The purpose of an abundance threshold is to downweigh overrepresented pollen taxa that may be present due to higher dispersal capabilities (50, 52).

Climate Estimates. We use decadal mean annual temperature (MAT) and decadal mean total annual precipitation (MAP) to represent the climatic niches of plant taxa, using climate data extracted from the debiased, downscaled SynTrace CCSM3 simulation (53–55). The paleoclimate dataset consists of climate data at the spatiotemporal resolution of decadal seasonal averages every 0.5° × 0.5° (latitude and longitude). For surface pollen samples, to maintain data consistency, we use the climate data for 1980 AD from the same dataset. MAT and MAP strongly correlate with all other climate variables under consideration, including min/max annual temperature/precipitation, summer/winter temperature/precipitation, and water deficit, with correlation coefficients > 0.7 (10, 15, *SI Appendix*, Table S13). Fossil records and modern observations also suggest that the SynTrace CCSM3 performs well in reconstructing abrupt temperature change after the last glaciation but less well in paleoprecipitation and climate seasonality reconstructions (53–55). We therefore select MAT and MAP to facilitate interpretation, to minimize covariation among variables, and to avoid potential false niche reconstructions due to inaccurate climate estimation.

Climatic Niches and the Available Environment. Hutchinson defined the fundamental niche of a taxon as the full set of environmental conditions where a species could survive (7). At any given time, the fundamental niche can be limited by the environmental conditions that are available to that taxon, known as the realized environmental space or the available environment (9). The overlap between a fundamental niche and the available environment is known as the potential niche of a taxon (9). The potential niche is further limited by intrinsic and extrinsic biotic factors, such as interspecific interactions and dispersal potential, resulting in the realized niche of the taxon (8, 9), a snapshot of the environmental conditions in which that taxon is found at a given time. Because we are only considering climatic components of the environment, we designate that we are considering the realized climatic niche of the taxa throughout. To evaluate climate fidelity and shifts in climatic realized niches in a manner that is fair, we must only consider the available environments across both time periods (27, 56). Methods used for the main text of the paper, niche overlap and niche similarity, consider the potential niches of the taxa when making calculations. Niche overlap only considers the overlap of available, potential niche space of the taxa. The null model in niche similarity assumes that species distribute randomly in the available environment but with the same kernel density as the observed niche. Calculations of niche equivalency, which is another statistical method to evaluate species niche conservatism, do not take the potential climatic niche into account. A discussion of its interpretation can be found in the *SI Appendix* (Niche equivalency, *SI Appendix*, Fig. S7 and Table S11).

Niche Overlap. Here, niche overlap describes the kernel-density-weighted overlap of two climatic realized niches calculated for adjacent time bins, only considering the aspect of the environment present during both time bins (19, 21). We use Schoener's overlap metric *D* to calculate niche overlap (19–21). Schoener's *D* statistic accounts for the overlap of two probability distributions (20),

$$D(p_{t_n}, p_{t_{n+1}}) = 1 - \frac{1}{2}\sum_i |p_{t_n,i} - p_{t_{n+1},i}|,$$

where p is the occurrence probability distribution of the taxon (i) in a time bin (t). Schoener's *D* ranges from 0 (no overlap) to 1 (identical). Here, we use kernel density to estimate the probability distribution of plant's realized climatic niche within an age bin.

We use the function *ecospat.niche.overlap* in the R package *ecospat* (57, 58) to calculate niche overlap. The climate associated with all pollen samples for a given age bin serves as the background climate, estimating the kernel density of a taxon's available environment for that age bin (9). When calculating the realized climatic niche overlap in the transition period, we additionally remove marginal niche space by using 95% of niche kernel densities. The calculated realized climatic niche overlaps of all plant taxa across all transition periods are in the *SI Appendix* (*SI Appendix*, Table S6 and Fig. S4).

Niche Similarity. Niche similarity can evaluate the statistical significance of observed niche overlaps given the available environments of two time periods. Niche similarity is a statistical method used to test the significance of niche conservatism by comparing the overlap of two observed niches with a bootstrapped null of simulated niche overlaps (19, 21, 57). Previously, this method has been used to evaluate the niche conservatism of sister taxa in a phylogenetic context (e.g., 59) or to study invasive species (e.g., 60). For these types of tests, niche conservatism is evaluated between two taxa or between two geographic regions, respectively. Here, we modify this statistical test to evaluate how conserved a realized climatic niche is across two time bins given the available climates for each of those time bins, evaluating the climate fidelity of the taxon.

We use *ecospat.niche.similarity.test* to perform the niche similarity test (57). The function first constructs a null distribution of simulated niche overlaps for the two time bins. To do this, the niche similarity test samples two simulated niches, one from the available climates of each of the two time periods (t_n and t_{n+1}). The kernel density distribution of each random niche is the same as its observed niche but shifted in available climate space (56–58, 61). The niche similarity test then calculates the overlaps for the two simulated niches using Schoener's *D* and the niche overlap calculation described above. We repeat this series of niche overlap simulations 1,000 times to create a null distribution of overlap *D* values. Using this null distribution, we determine whether the two observed niches in the transition periods are more similar than random, indicating climate fidelity. If the observed niche overlap falls below the significance threshold (fifth percentile or first percentile) of the random niche overlaps, the observed niche overlap is significantly greater than a random niche overlap. This suggests that the niches are convergent and that the taxon exhibits climate fidelity for that transition period. We use "significant" to indicate significance at the ≤0.01 level, "marginal significance" to indicate significance between 0.05 and 0.01, and "not significant" to indicate $P > 0.05$ (Fig. 2*A*).

Sample Size Sensitivity Test. We perform five sample size sensitivity tests to analyze the effect of pollen sample sizes on the calculation of niche overlap. Pineda-Munoz et al. (10) suggests that the niche overlap analysis is reliable when sample size ≥ 20. In our work, we pool pollen samples into four 4,000-y time bins from 18 to 2 ka to confirm that there are at least 20 samples for each

taxon in each time bin, especially in the DG bin (18–14 ka) (*SI Appendix*, Table S12). We divide the time after 2 ka into 2 ka–1950 AD and 1950 AD–present because we want to analyze the influences of humans on niche overlaps. The year 1950 AD marks a significant increase in human activity in North America because it marks the spread of modern cities (62). We think, rather than different time bin lengths, different sample sizes play a more important role in calculating niche overlaps. Shorter time bins may not leave plants enough time to migrate and to track climate change, leading to lower niche overlaps. However, the average niche overlap between the two shortest time bins (2 ka–1950 AD and after 1950 AD) are still high (>0.6) and exhibit significant climate fidelity in plants across this period. Further, average niche overlap in these shorter time bins is even higher than the average niche overlap in the deglacial transition period between two longer time bins (18–14 ka and 14–10 ka, Fig. 2*B*). The high niche overlap in the recent transition period is more likely to be biased by the large sample size in the recent time bins.

We bootstrap N samples per age bin per plant taxa 100 times for a sample size sensitivity test, where $n = 20$, 50, 100, and all samples, separately. Because the age bin 18–14 ka contains the least samples in all age bins (431 samples out of 17,550 samples), we also design a sample size sensitivity test by bootstrapping 431 samples across all plants in each of the other age bins 100 times. This final test limits all age bins' sample sizes to the same no. to reduce the effect of low sample sizes in the 18–14 ka time bin. Results suggest that, although the absolute magnitude of niche overlap changes, the trends through time do not differ much across our five sample size sensitivity tests (*SI Appendix*, Fig. S8). Herein, we report the result using all samples to approximate the correct overlap magnitude while maintaining consistent trends across taxa. However, we limit the minimum sample size per age bin per plant taxa to 50 (*SI Appendix*, Table S12). This relatively high and conserved minimum sample size no. further reduces the effect from sample size and increases the reliability of our niche overlap analysis.

Niche Overlap and Climate Change. We compare plants' niche overlaps between transitions with the magnitude of climate change across each transition. For each taxon, we calculate Pearson's r between niche overlaps and the magnitudes of background temperature change and background precipitation change, separately, for the five transition periods. The background climate is sampled from all $0.5° \times 0.5°$ grid cells across North America except ice sheets, and average differences are calculated. If climate change affects plants' niche overlaps, the niche overlap should be small when the magnitude of climate change is high, and the Pearson's r should be negative. Pearson's r values are in the *SI Appendix* (*SI Appendix*, Table S7).

Plant Climate Propensity. We divide plant taxa into two groups based on their temperature and precipitation preferences. We calculate the climatic niche centroids of plant taxa from the last 18,000 y (*SI Appendix*, Table S8). We then calculate the ratio of MAP to MAT for each plant taxon, where the temperature and precipitation are scaled separately to the range 0–1 (Fig. 2*B*, *Inset*). We divide plant taxa into two groups based on the precipitation/temperature ratios: *Tsuga*, *Abies*, *Alnus*, *Picea*, *Betula*, and *Fagus* compose a cold and wet taxa group for which the precipitation to temperature ratio is higher than 0.5. *Fraxinus*, *Quercus*, *Pinus*, Cupressaceae, *Ulmus*, Cyperaceae, *Salix*, Poaceae, *Artemisia*, and Amaranthaceae compose the warm and dry taxa group (Fig. 2*A*). We plot the niche overlap values for cold/wet and warm/dry plant taxa over time to evaluate whether one group showed consistently higher niche overlap than the other (Fig. 2*B*).

Migration Distance. We estimate the migration distances of plant taxa across transition periods by calculating changes in the centroids of the geographic kernel densities of each taxon. These migration distances do not consider elevation changes or geographic barriers. However, given the propensity of propagules to exhibit LDD, geographic barriers may not play a large role in the dispersal of many plants (25, 26, 63). Our calculated migration distances give a simple, though rough, estimation of plants' dispersal ability. The calculated migration distances are in *SI Appendix* (*SI Appendix*, Table S9). We calculate the mean plant migration distance and divided taxa into long-migrating taxa (top 50%) and short-migrating taxa (lower 50%; Fig. 3*A*, *Inset*). We plot the niche overlap values for long-migrating versus short-migrating plant taxa over time to evaluate whether one group showed consistently higher niche overlap than the other (Fig. 3*A*). We perform t tests to compare the niche overlap values of the two groups both across all transitions and across the two transitions that experienced significant climate shifts (the DG and the early Holocene; Fig. 3 *B* and *C*).

Climate Fidelity Hotspots. We finally calculate climate fidelity scores for surface pollen sites, which represent modern plant communities. To do so, we first calculate the level of climate fidelity significance (significant, marginally significant, or not significant; see above) for each plant taxon over the last 18,000 y. Each taxon's climate fidelity score is a sum of its climate fidelity significance scores across all transition periods. Significant climate fidelity for a transition period counts for one point, marginally significant climate fidelity counts for 0.5 points, and nonsignificance contributes zero points. Climate fidelity scores of each plant taxon are in the *SI Appendix* (*SI Appendix*, Table S10). We then calculate the climate fidelity scores of surface pollen sites based on their modern plant composition and climate fidelity scores. The calculated site climate fidelity scores range from 4.5 to 59.0 (*SI Appendix*, Fig. S5). We also divide the sites into four categories based on their climate fidelity scores: hotspots (top 25%) where climate fidelity score > 37.0, moderate-high-climate-fidelity sites (25–50%) where climate fidelity score > 28.5 and ≤ 37.0, moderate-low-climate-fidelity sites (50–75%) where climate fidelity score > 23.5 and ≤ 28.5, and low-climate-fidelity sites (coldspots; bottom 75%) where climate fidelity score ≤ 23.5 (Fig. 4*A*). We compare climate fidelity hotspots and coldspots to regions of climate resilience and regions of connectivity/nonconnectivity using ArcGIS as calculated by The Nature Conservancy (64, 65) (Fig. 4*B* and *SI Appendix*, Fig. S6). They calculated resilience scores across the United States using an algorithm that combines current land use, topographic complexity, and local connectivity. Climate resilience around climate fidelity hotspots and coldspots are the values of groups of pixels around the sites. We also extract the information of connectivity/nonconnectivity at the sites from the layer of categorical connectivity and climate flow (64, 65). The Nature Conservancy connectivity layer is mainly dominated by land use and natural barriers.

Data, Materials, and Software Availability. R scripts, data tables, and outputs can be found on Zenodo: 10.5281/zenodo.6596636.

[R scripts and data tables] data have been deposited in [ClimateFidelity] (10.5281/zenodo.6596636) (66).

ACKNOWLEDGMENTS. The work was supported by NSF grants BIO DEB PCE 1655898 and GEO EAR SGP 1945013. Data were obtained from the Neotoma Paleoecology Database (https://www.neotomadb.org). The work of data contributors, data stewards, and the Neotoma community is gratefully acknowledged. We sincerely thank the editors for their efforts on the special issue. We also would like to thank Kimberly Hall at The Nature Conservancy and other two anonymous reviewers for their constructive comments, which helped us to improve the manuscript. We thank the members of the Spatial Ecology and Paleontology Lab at Georgia Tech and other authors from this PNAS Special Feature, particularly Michelle Lawing and Mark Anderson, for their suggestions on the project.

1. J. J. Lawler, A. S. Ruesch, J. D. Olden, B. H. McRae, Projected climate-driven faunal movement routes. *Ecol. Lett.* **16**, 1014–1022 (2013).
2. D. D. Ackerly, Community assembly, niche conservatism, and adaptive evolution in changing environments. *Int. J. Plant Sci.* **164**, S165–S184 (2003).
3. P. B. Pearman, A. Guisan, O. Broennimann, C. F. Randin, Niche dynamics in space and time. *Trends Ecol. Evol.* **23**, 149–158 (2008).
4. J. J. Wiens, C. H. Graham, Niche conservatism: Integrating evolution, ecology, and conservation biology. *Annu. Rev. Ecol. Evol. Syst.* **36**, 519–539 (2005).
5. D. Fraser *et al.*, Investigating biotic interactions in deep time. *Trends Ecol. Evol.* **36**, 61–75 (2021).
6. J. L. McGuire, J. J. Lawler, B. H. McRae, T. A. Nuñez, D. M. Theobald, Achieving climate connectivity in a fragmented landscape. *Proc. Natl. Acad. Sci. U.S.A.* **113**, 7195–7200 (2016).
7. G. E. Hutchinson, Concluding remarks. *Cold Spring Harbor Symposia on Quantitative Biology* **22**, 415–427 (1957).
8. A. T. Peterson *et al.*, *Ecological Niches and Geographic Distributions* (Princeton University Press, 2011).
9. S. T. Jackson, J. T. Overpeck, Responses of plant populations and communities to environmental changes of the late Quaternary. *Paleobiology* **26**, 194–220 (2000).

10. S. Pineda-Munoz, Y. Wang, K. Lyons, A. B. Tóth, J. McGuire, Mammal species occupy different climates following the expansion of human impacts. *Proc. Natl. Acad. Sci. U.S.A.* **118, e1922859118** (2021).
11. S. D. Veloz *et al.*, No-analog climates and shifting realized niches during the late Quaternary: Implications for 21st-century predictions by species distribution models. *Glob. Change Biol.* **18**, 1698–1713 (2012).
12. C. A. Knight *et al.*, Community assembly and climate mismatch in late Quaternary eastern North American pollen assemblages. *Am. Nat.* **195**, 166–180 (2020).
13. J. S. McLachlan, J. S. Clark, P. S. Manos, Molecular indicators of tree migration capacity under rapid climate change. *Ecology* **86**, 2088–2098 (2005).
14. J. W. Williams, B. N. Shuman, T. Webb, P. J. Bartlein, P. L. Leduc, Late-Quaternary vegetation dynamics in North America: Scaling from taxa to biomes. *Ecol. Monogr.* **74**, 309–334 (2004).
15. Y. Wang, B. R. Shipley, D. A. Lauer, R. M. Pineau, J. L. McGuire, Plant biomes demonstrate that landscape resilience today is the lowest it has been since end-Pleistocene megafaunal extinctions. *Glob. Chang. Biol.* **26**, 5914–5927 (2020).
16. S. R. Loarie *et al.*, The velocity of climate change. *Nature* **462**, 1052–1055 (2009).
17. S. N. Aitken, S. Yeaman, J. A. Holliday, T. Wang, S. Curtis-McLane, Adaptation, migration or extirpation: Climate change outcomes for tree populations. *Evol. Appl.* **1**, 95–111 (2008).
18. J. W. Williams, D. M. Post, L. C. Cwynar, A. F. Lotter, A. J. Levesque, Rapid and widespread vegetation responses to past climate change in the North Atlantic region. *Geology* **30**, 971–974 (2002).
19. O. Broennimann *et al.*, Measuring ecological niche overlap from occurrence and spatial environmental data. *Glob. Ecol. Biogeogr.* **21**, 481–497 (2012).
20. T. W. Schoener, Nonsynchronous spatial overlap of lizards in patchy habitats. *Ecology* **51**, 408–418 (1970).
21. D. L. Warren, R. E. Glor, M. Turelli, Environmental niche equivalency versus conservatism: Quantitative approaches to niche evolution. *Evolution* **62**, 2868–2883 (2008).
22. D. Nogués-Bravo *et al.*, Phenotypic correlates of potential range size and range filling in European trees. *Perspect. Plant Ecol. Evol. Syst.* **16**, 219–227 (2014).
23. M. G. Anderson *et al.*, *Resilient and Connected Landscapes for Terrestrial Conservation* (The Nature Conservancy, Eastern Conservation. Science, Eastern Regional Office, Boston, MA, 2016), pp. 1–149.
24. M. Anderson *et al.*, Identifying resilient and connected landscapes to serve as conservation priorities in a dynamically changing world. *Proc. Natl. Acad. Sci. U.S.A.* (2022).
25. J. S. Clark, Why trees migrate so fast: Confronting theory with dispersal biology and the paleorecord. *Am. Nat.* **152**, 204–224 (1998).
26. R. Nathan, Long-distance dispersal of plants. *Science* **313**, 786–788 (2006).
27. G. S. Antell, I. S. Fenton, P. J. Valdes, E. E. Saupe, Thermal niches of planktonic foraminifera are static throughout glacial-interglacial climate change. *Proc. Natl. Acad. Sci. U.S.A.* **118**, e2017105118 (2021).
28. L. B. Brubaker, P. M. Anderson, M. E. Edwards, A. V. Lozhkin, Beringia as a glacial refugium for boreal trees and shrubs: New perspectives from mapped pollen data. *J. Biogeogr.* **32**, 833–848 (2005).
29. A. M. Thomson, C. W. Dick, S. Dayanandan, A similar phylogeographical structure among sympatric North American birches (Betula) is better explained by introgression than by shared biogeographical history. *J. Biogeogr.* **42**, 339–350 (2015).
30. G. L. Jacobson Jr., T. Webb III, E. C. Grimm, Patterns and rates of vegetation change during the deglaciation of eastern North America. *North Am. Adjac. Ocean. Dur. Last Deglaciation* **3**, 277–288 (1987).
31. B. J. Seliger, B. J. McGill, J. C. Svenning, J. L. Gill, Widespread underfilling of the potential ranges of North American trees. *J. Biogeogr.* **48**, 359–371 (2021).
32. J. L. Gill, J. W. Williams, S. T. Jackson, K. B. Lininger, G. S. Robinson, Pleistocene megafaunal collapse, novel plant communities, and enhanced fire regimes in North America. *Science* **326**, 1100–1103 (2009).
33. A. M. Lawing, J. L. Blois, K. C. Maguire, S. J. Goring, J. L. McGuire, Paleo-occupancy models reveal regional differences in detectability and improve abundance estimations. *Quat. Sci. Rev. 253, 106747 (2021).*
34. J. S. McLachlan, J. S. Clark, Reconstructing historical ranges with fossil data at continental scales. *For. Ecol. Manage.* **197**, 139–147 (2004).
35. R. K. Booth *et al.*, A severe centennial-scale drought in midcontinental North America 4200 years ago and apparent global linkages. *Holocene* **15**, 321–328 (2005).
36. H. Weiss, Global megadrought, societal collapse and resilience at 4.2–3.9 ka BP across the Mediterranean and west Asia. *PAGES* **24**, 62–63 (2016).
37. J. P. Marsicek, B. Shuman, S. Brewer, D. R. Foster, W. W. Oswald, Moisture and temperature changes associated with the mid-Holocene Tsuga decline in the northeastern United States. *Quat. Sci. Rev.* **80**, 129–142 (2013).
38. Y. Wang *et al.*, Pronounced variations in Fagus grandifolia abundances in the Great Lakes region during the Holocene. *Holocene* **26**, 578–591 (2016).
39. G. M. MacDonald *et al.*, Prolonged California aridity linked to climate warming and Pacific sea surface temperature. *Sci. Rep.* **6**, 33325 (2016).
40. D. M. Nelson, F. S. Hu, Patterns and drivers of Holocene vegetational change near the prairie-forest ecotone in Minnesota: Revisiting McAndrews' transect. *New Phytol.* **179**, 449–459 (2008).
41. M. B. Soons, J. M. Bullock, Non-random seed abscission, long-distance wind dispersal and plant migration rates. *J. Ecol.* **96**, 581–590 (2008).
42. R Core Team, R: A language and environment for statistical computing. R Foundation for Statistical Computing, Vienna, Austria (2021).
43. J. W. Williams *et al.*, The Neotoma Paleoecology Database, a multiproxy, international, community-curated data resource. *Quat. Res.* **89**, 156–177 (2018).
44. S. Goring *et al.*, neotoma: A programmatic interface to the Neotoma Paleoecological Database. *Open Quat.* **1**, 2 (2015).
45. J. Whitmore *et al.*, Modern pollen data from North America and Greenland for multi-scale paleoenvironmental applications. *Quat. Sci. Rev.* **24**, 1828–1848 (2005).
46. Y. Wang, S. J. Goring, J. L. McGuire, Bayesian ages for pollen records since the last glaciation in North America. *Sci. Data* **6**, 176 (2019).
47. S. J. Goring, A. Dawson, M. A. Stegner, Y. Wang, Bulk baconizing (2019). https://doi.org/10.5281/zenodo.2545891.
48. B. L. Otto-Bliesner *et al.*, Climate variability and change since 850 CE: An ensemble approach with the Community Earth System Model. *Bull. Am. Meteorol. Soc.* **97**, 735–754 (2016).
49. Y. Wang *et al.*, Mechanistic modeling of environmental drivers of woolly mammoth carrying capacity declines on St. Paul Island. *Ecology* **99**, 2721–2730 (2018).
50. J. W. Williams, R. L. Summers, T. Webb, Applying plant functional types to construct biome maps from eastern North American pollen data: Comparisons with model results. *Quat. Sci. Rev.* **17**, 607–627 (1998).
51. J. W. Williams, T. Webb III, P. H. Richard, P. Newby, Late Quaternary biomes of Canada and the eastern United States. *J. Biogeogr.* **27**, 585–607 (2000).
52. C. Prentice, J. Guiot, B. Huntley, D. Jolly, R. Cheddadi, Reconstructing biomes from palaeoecological data: A general method and its application to European pollen data at 0 and 6 ka. *Clim. Dyn.* **12**, 185–194 (1996).
53. F. He *et al.*, Northern Hemisphere forcing of Southern Hemisphere climate during the last deglaciation. *Nature* **494**, 81–85 (2013).
54. Z. Liu *et al.*, Transient simulation of last deglaciation with a new mechanism for Bølling-Allerød warming. *Science* **325**, 310–314 (2009).
55. D. J. Lorenz, D. Nieto-Lugilde, J. L. Blois, M. C. Fitzpatrick, J. W. Williams, Downscaled and debiased climate simulations for North America from 21,000 years ago to 2100AD. *Sci. Data* **3**, 160048 (2016).
56. A. T. Peterson, Ecological niche conservatism: A time-structured review of evidence. *J. Biogeogr.* **38**, 817–827 (2011).
57. O. Broennimann, V. Di Cola, A. Guisan, ecospat: Spatial ecology miscellaneous methods. *R Package* version **3**.2 (2021).
58. V. Di Cola *et al.*, ecospat: An R package to support spatial analyses and modeling of species niches and distributions. *Ecography* **40**, 774–787 (2017).
59. D. da Silva, A. E. Aires, J. P. Zurano, M. A. Olalla-Tárraga, P. A. Martinez, Changing only slowly: The role of phylogenetic niche conservatism in Caviidae (Rodentia) speciation. *J. Mamm. Evol.* **27**, 713–721 (2020).
60. C. Liu, C. Wolter, W. Xian, J. M. Jeschke, Most invasive species largely conserve their climatic niche. *Proc. Natl. Acad. Sci. U.S.A.* **117**, 23643–23651 (2020).
61. A. T. Peterson, J. Soberón, V. Sánchez-Cordero, Conservatism of ecological niches in evolutionary time. *Science* **285**, 1265–1267 (1999).
62. D. E. Shi, G. B. Tindall, *America: A Narrative History, Brief* (W. W. Norton & Company, ed. 10, 2016).
63. I. Hanski, Metapopulation dynamics. *Nature* **396**, 41–49 (1998).
64. M. G. Anderson *et al.*, Resilient sites for terrestrial conservation in the southeast region. The Nature Conservancy, Eastern Conservation Science, 127 (2014).
65. The Nature Conservancy, Resilient and connected network: Datasets for the conterminous U.S. http://www.conservationgateway.org/ConservationPractices/ClimateChange/Pages/RCN-Downloads.aspx. ccessed 23 December 2021.
66. Y. Wang, S. Pineda-Munoz, J. L. McGuire, Plants maintain climate fidelity in the face of dynamic climate change. Zenodo. https://zenodo.org/record/6596636#.YvvH3HZBy3A. Deposited 31 May 2022.